Abstracting ENSO Spatial Patterns' Impact on Atlantic Tropical Cyclone Seasonal Frequency

2012-05-14

Abstract

1 Introduction

Understanding and predicting tropical cyclone (TC) activity is of significant scientific and societal interest.

One of the environmental factors that influence large scale circulation globally are the Pacific Ocean sea surface temperatures (SSTs). In fact, research interested in predicting seasonal TC activity with reasonable lead times have attributed an increase in predictive power to an increased ability to predict Pacific SSTs [13]. The warming anomalies of sea surface temperatures (SSTs) along the near-equatorial Pacific Ocean have well documented global long-range weather teleconnections from rainfall in southern India to mudslides in the western United States. This quasi-periodic cycle (2-7 years) of warming and cooling known as the El-Niño Souther Oscillation (ENSO) is associated with anomalous atmospheric circulation and alterations to the Eastern Pacific thermocline (the subsurface boundary between upper warm waters and deep cool waters). During its warm, El-Niño (EN) phase, the equatorial Pacific Ocean experiences weak easterly winds causing an increase in Eastern Pacific SSTs, that in turn alters the atmospheric zonal (Walker) circulation, generally resulting in prevailing westerlies. ENSO's cold, La Niña (LN) phase, is characterized by the opposite atmospheric conditions – with cold SST anomalies along the Eastern Pacific and warm ones near the Western Pacific as a result of prevailing easterly winds (see Figure 1). The mechanisms that control the reversal to the opposite LN phase are not fully understood [10, 14]. Recent research has suggested that to fully capture ENSO activity, it is no longer sufficient to monitor the warm and cold phases in the Eastern Pacific. Instead, warming patterns in the Central Pacific must be monitored as well [1]. Warming in the Central Pacific, known as El Niño Modoki, where a warm waters are surrounded by cold ones has been observed with increased frequency since the 1990s. Such changes have been attributed to anthropogenic global warming [19] as well as natural climate variability [18].

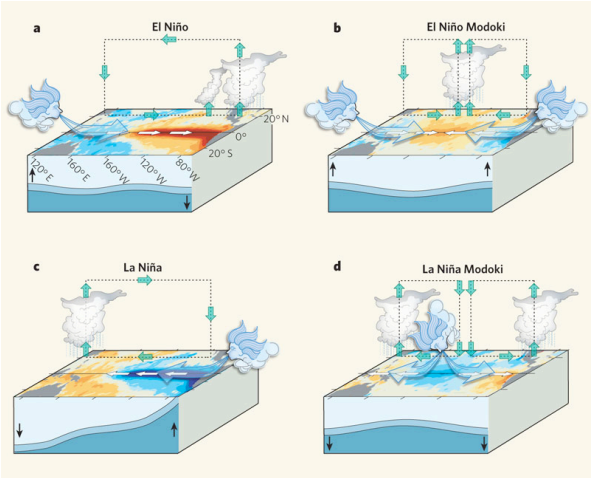

Figure 1: (a), An El Niño event is produced when the easterly winds weaken; sometimes, in the west, westerlies prevail. This condition is categorized by warmer than normal sea surface temperatures (SSTs) in the east of the ocean, and is associated with alterations in the thermocline and in the atmospheric circulation that make the east wetter and the west drier. (b), An El Niño Modoki event is an anomalous condition of a distinctly different kind. The warmest SSTs occur in the central Pacific, flanked by colder waters to the east and west, and are associated with distinct patterns of atmospheric convection. (c), (d), The opposite (La Niña) phases of the El Niño and El Niño Modoki respectively. Image and caption used for illustration purposes only taken from [2]

One of the ENSO teleconnections is with North Atlantic tropical cyclone (TC) activity. Enhanced convection as a result of anomalous Pacific Ocean warming is associated with strong westerly upper tropospheric wind over the Caribbean basin and tropical Atlantic, resulting in low TC activity during EN events and high TC activity LN. Other studies have suggested that ENSO impact Atlantic TC activity via tropospheric warming [15]. The influence of ENSO on Atlantic TCs is well documented [8, 4, 5, 11], however due to the large amplitude variations of seasonal counts, the difference in Atlantic TC activity based on the various phases of ENSO is not obvious (see Figure 2).

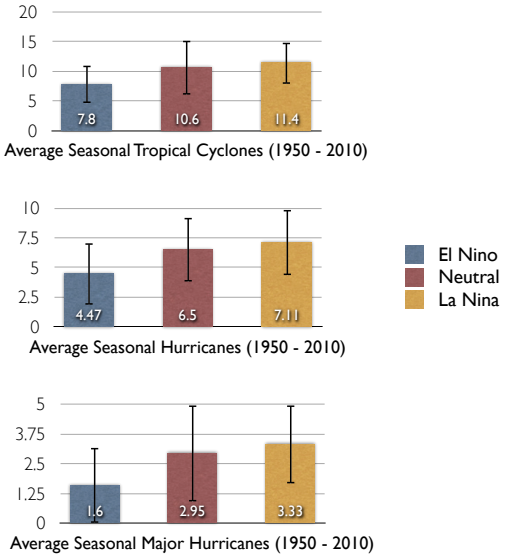

Figure 2: The $1950 - 2010$ seasonal mean Atlantic tropical cyclones (top), hurricanes (middle), and major hurricane (bottom) counts for El-Niño, neutral, and La Niña years. Vertical bars denote standard deviation. The overlap between between bars across categories make distinguishing between Atlantic TC activity based on the phase of ENSO ambiguous.

Given its long-range teleconnections, as well as ENSO being the most dominant feature of cyclic climate variability on subdecadal timescales, effectively abstracting and predicting Pacific Ocean warming anomalies has been a subject of active research. ENSO has been quantified using simple warming-based indices where SST anomalies are averaged over regions in the Pacific. Such indices include the Nino 1+2 (0-10S, 90-80W), Nino 3 (5N-5S, 150-90W), Nino 4 (5N-5S, 160E-150W), and Nino 3.4 (5N-5S, 170-120W). Some studies have suggested such indices do not capture ENSO's nature and evolution. Subsequently, more elaborate indices were developed some of which were linear combinations of the above-mentioned indices [16], while others have proposed indices using transformed data or nonlinear combination of indices [12]. Despite the varying

	TCs	Major Hurricanes	ACE	PDI	NTC
Spatial ENSO	-0.44	-0.39	-0.40	-0.39	-0.43
NINO 1+2	-0.07	-0.13	0.01	0.02	-0.04
NINO 3.4	-0.07	-0.11	0.01	0.02	0.03
NINO 3	0.04	-0.08	0.06	0.08	0.03
NINO 4	0.09	-0.08	0.08	0.11	0.10

Table 1: Linear correlation coefficients between January-April mean SSTs of traditional warming-based ENSO indices as well as the January-April Spatial ENSO index and August-October Atlantic TC activity. Our Spatial ENSO index significantly outperforms traditional indices.

degrees of complexity, the majority of works attempting to capture ENSO focus on the intensity of warming in a given geographical region. However using such indices provide little additional skill in predicting Atlantic TC activity. An increasing number of studies have suggested changes in the spatial warming patterns of the Pacific Ocean and some have linked those changes U.S. hurricane landfall probabilities [9]. We propose that based on such results, the spatial distribution of Pacific Ocean warming might provide better predictive insights into ENSO-Atlantic TC activity better than warming anomalies alone. We propose a distance-based ENSO index that tracks the location of maximum near-tropical Pacific warming anomaly instead of its absolute warming.

1.1 ENSO Spatial Index

Given the limited insight traditional (warming) ENSO indices provide in forecasting seasonal hurricane activity, we proposal a spatial ENSO index that monitors the spatial distribution of Pacific Ocean warming. For each season, we search for the maximum positive warming anomaly in regions of size comparable to that of warming-based ENSO indices. The highest warming region is selected by searching the Northern Tropical Pacific ($0 - 30^\circ$ N). The time series of the location of the highest warming region is then correlated with various quantities that communicate August-October Atlantic TC activity: number of tropical cyclones, number of major hurricanes, potential dissipation index (PDI) [6], accumulated cyclone energy (ACE) [3], and net tropical cyclone energy (NTC) [7].

Tables **??** through **??** show the linear correlation coefficients between August-October TC Atlantic TC activity and our ENSO spatial index for Feb-April, April-June, and August-October respectively. In all cases our spatial ENSO index correlates better than traditional warming-based indices. The improvements increase as we increase lead time, with April lead times improving by more than an order of magnitude. This improvement is because traditional ENSO indices suffer from a "predictability barrier" that make it difficult to use them to predict TC activity before June [17].

	TCs	Major Hurricanes	ACE	PDI	NTC
Spatial ENSO	-0.53	-0.48	-0.36	-0.34	-0.40
NINO 1+2	-0.23	-0.32	-0.25	-0.26	-0.28
NINO 3.4	-0.23	-0.44	-0.25	-0.26	-0.29
NINO 3	-0.28	-0.40	-0.28	-0.29	-0.31
NINO 4	-0.10	-0.27	-0.10	-0.08	-0.09

Table 2: Linear correlation coefficients between April-June mean SSTs of traditional warming-based ENSO indices as well as the January-April Spatial ENSO index and August-October Atlantic TC activity. Our Spatial ENSO index significantly outperforms traditional indices.

	TCs	Major Hurricanes	ACE	PDI	NTC
Spatial ENSO	-0.62	-0.57	-0.69	-0.67	-0.70
NINO 1+2	-0.55	-0.47	-0.44	-0.42	-0.49
NINO 3.4	-0.55	-0.51	-0.44	-0.42	-0.46
NINO 3	-0.51	-0.50	-0.46	-0.44	-0.49
NINO 4	-0.34	-0.48	-0.33	-0.32	-0.35

Table 3: Linear correlation coefficients between July-October mean SSTs of traditional warming-based ENSO indices as well as the January-April Spatial ENSO index and August-October Atlantic TC activity. Our Spatial ENSO index significantly outperforms traditional indices.

1.2 Sensitivity Tests

To validate our results, we test the sensitivity of our results to the month ranges used to build the index, the size of the ENSO box used, the size of the search space, and the months used as TC season. As it can be seen from the figures below, our results are stable with respect to parameter choice, except for search space where the correlations chance drastically based on which region we search.

1.3 Box Size Sensitivity Results

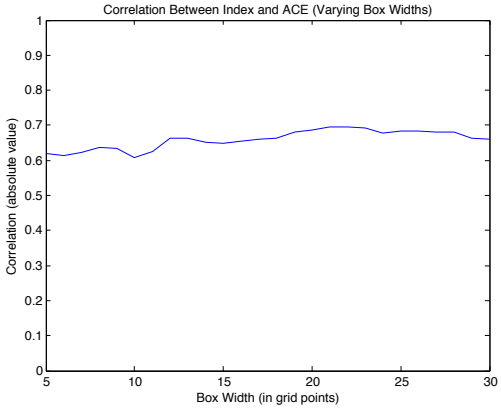

Figure 3: Corr Index vs. ACE

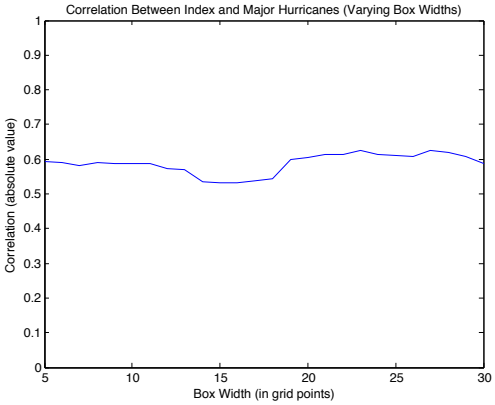

Figure 4: Corr Index vs. Major Hurricanes

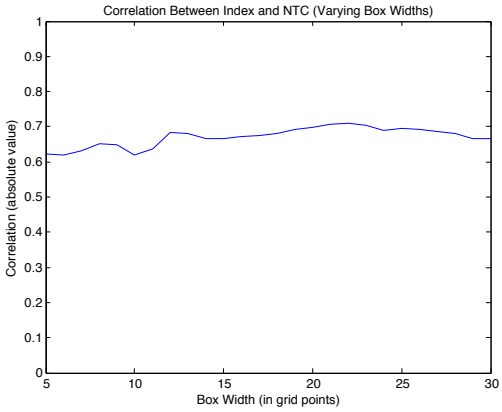

Figure 5: Corr Index vs. NTC

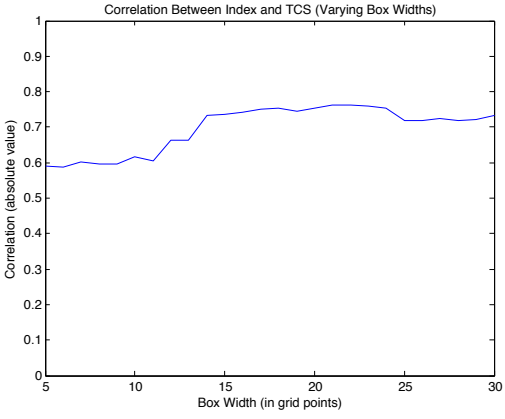

Figure 6: Corr Index vs. TCs

1.4 Varying Month Ranges

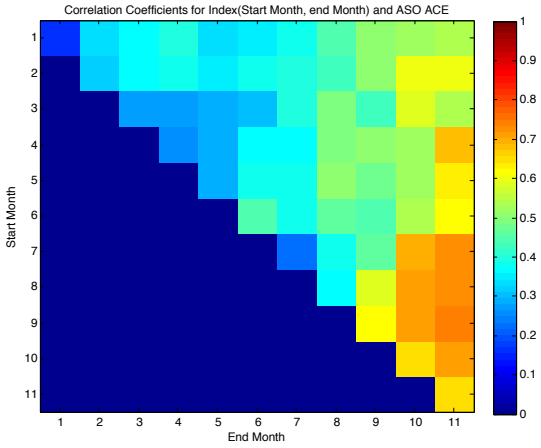

Figure 7: Corr Index vs. ACE

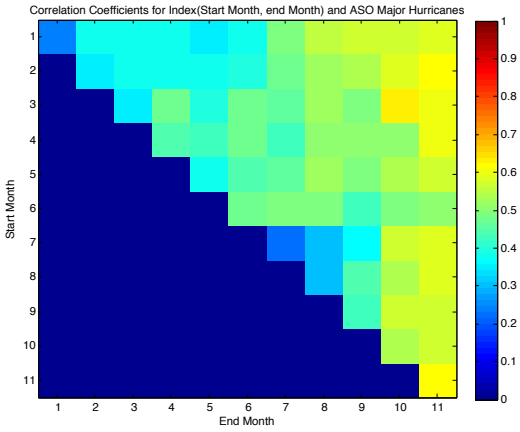

Figure 8: Corr Index vs. Major Hurricanes

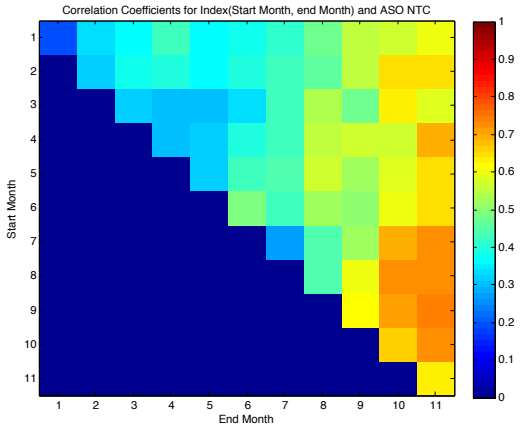

Figure 9: Corr Index vs. NTC

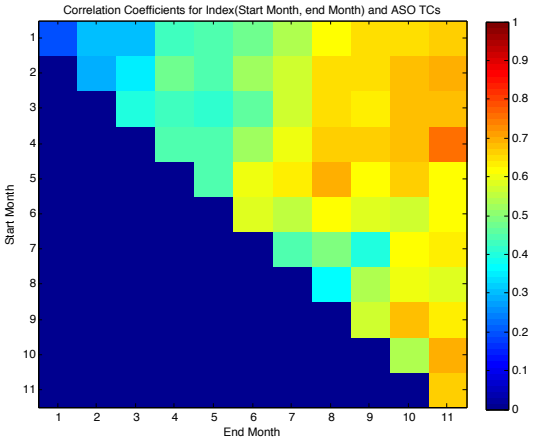

Figure 10: Corr Index vs. TCs

1.5 Varying Search Space (North and South Hemispheres)

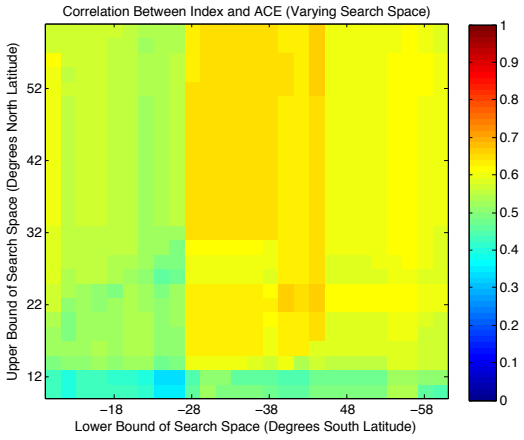

Figure 11: Corr Index vs. ACE

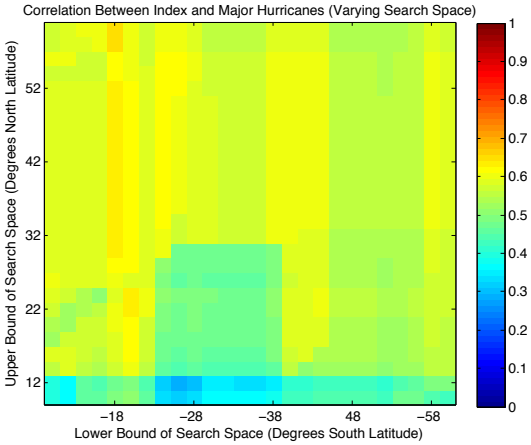

Figure 12: Corr Index vs. Major Hurricanes

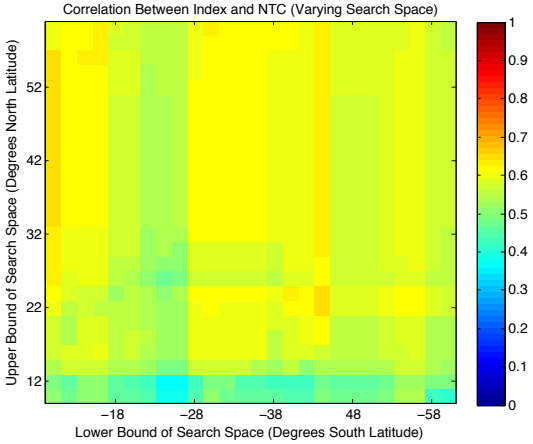

Figure 13: Corr Index vs. NTC

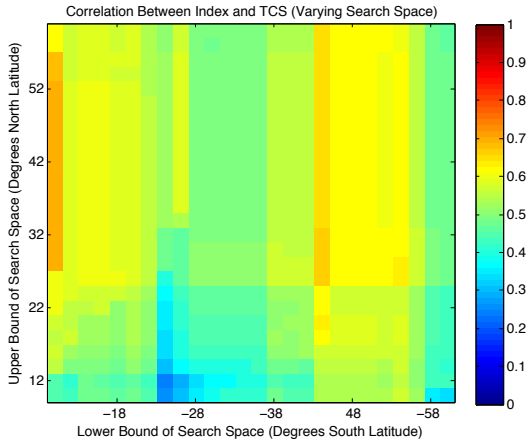

Figure 14: Corr Index vs. TCs

1.6 Varying Search Space (North Hemisphere)

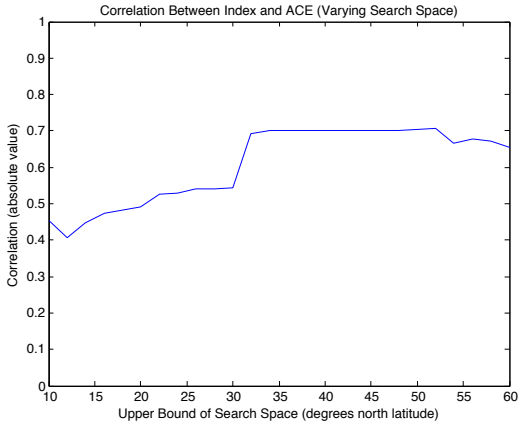

Figure 15: Corr Index vs. ACE

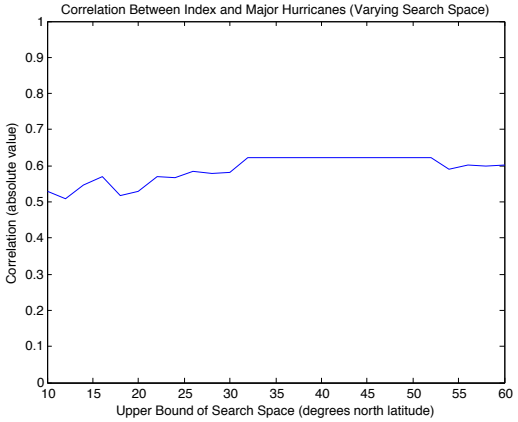

Figure 16: Corr Index vs. Major Hurricanes

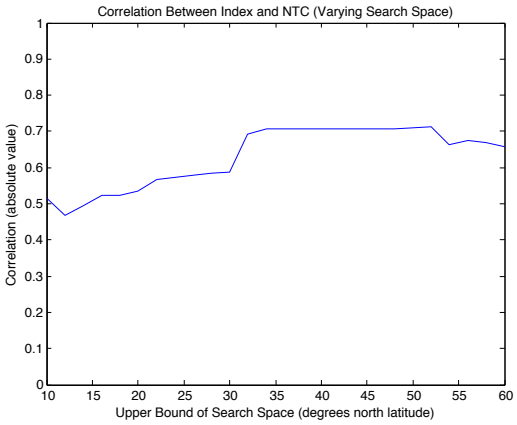

Figure 17: Corr Index vs. NTC

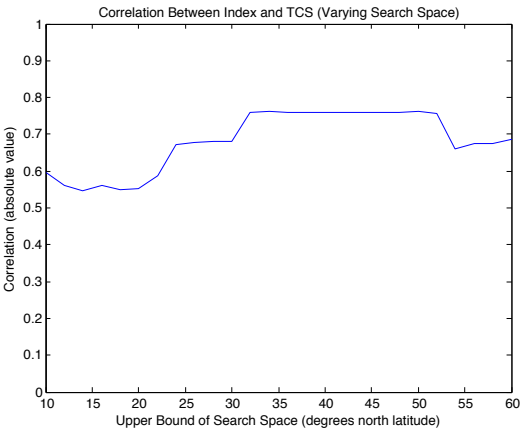

Figure 18: Corr Index vs. TCs

1.7 Varying Hurricane Season

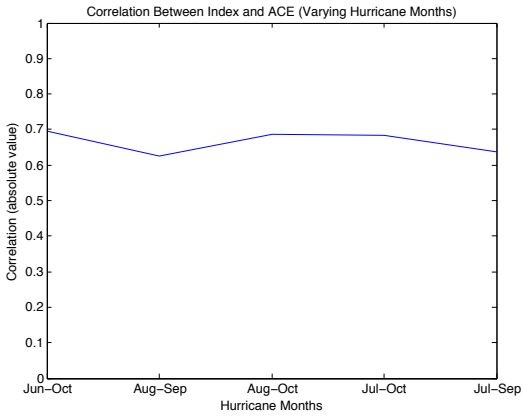

Figure 19: Corr Index vs. ACE

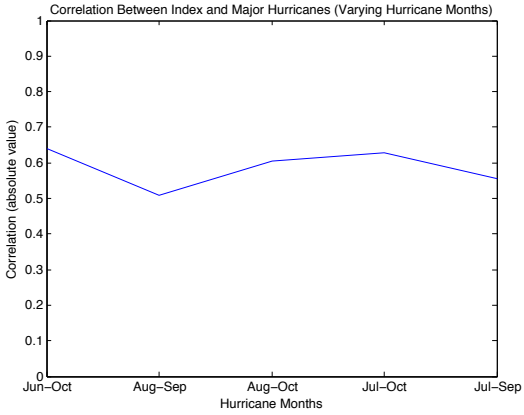

Figure 20: Corr Index vs. Major Hurricanes

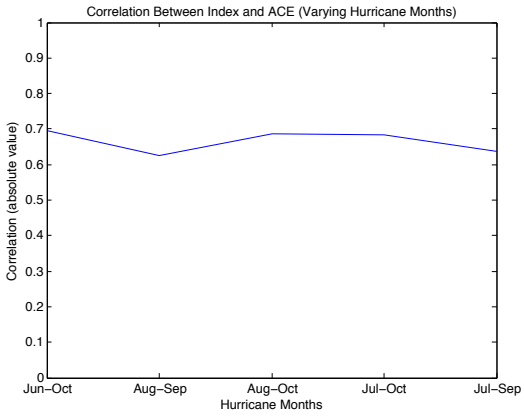

Figure 21: Corr Index vs. ACE

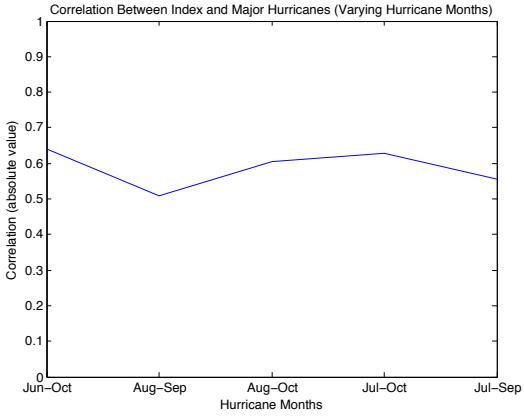

Figure 22: Corr Index vs. Major Hurricanes

2 Difference Composite Maps

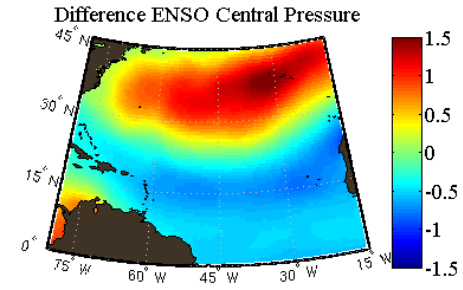

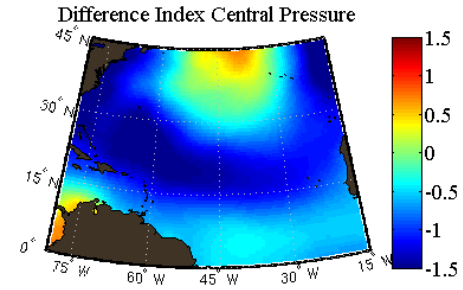

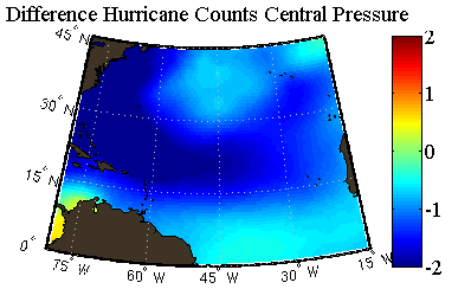

Figure 23: Diff Pressure Composites

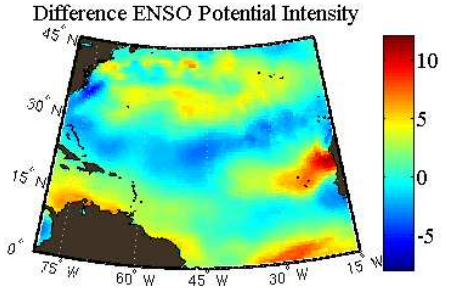

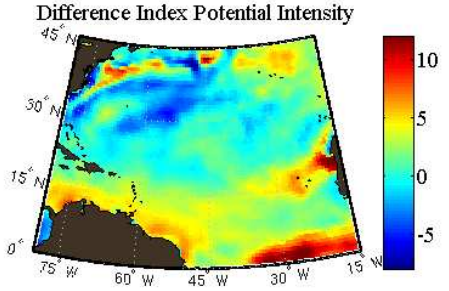

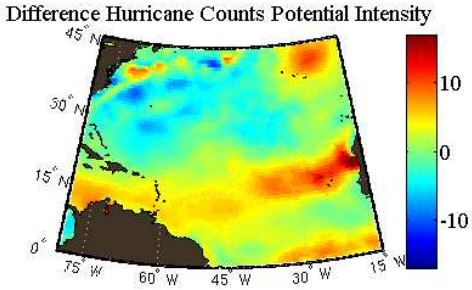

Figure 24: Diff PI Composites

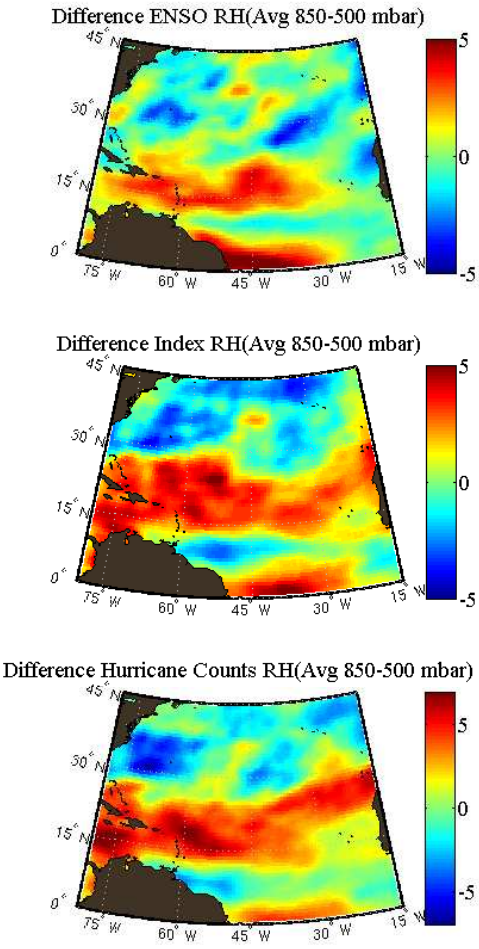

Figure 25: Diff Relative Humidity

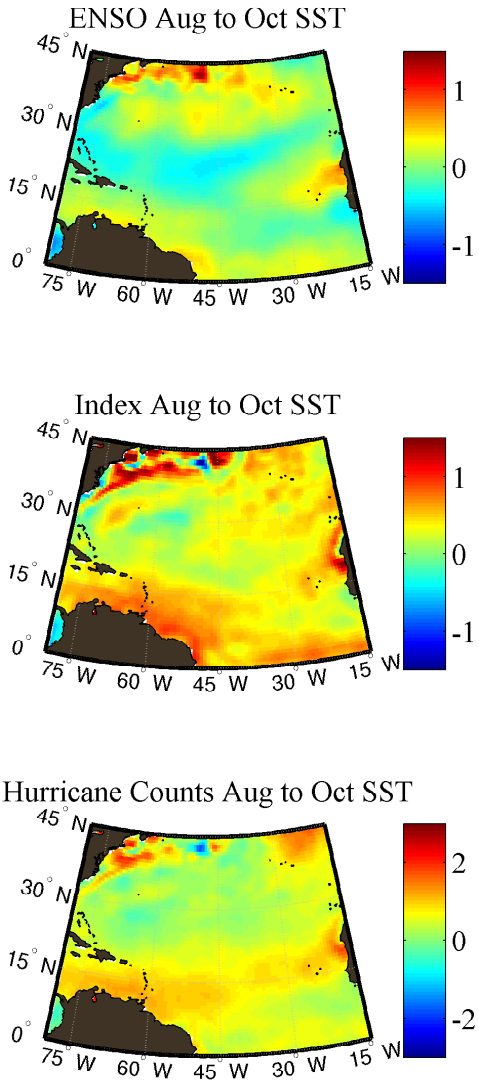

Figure 26: Diff SST Composites

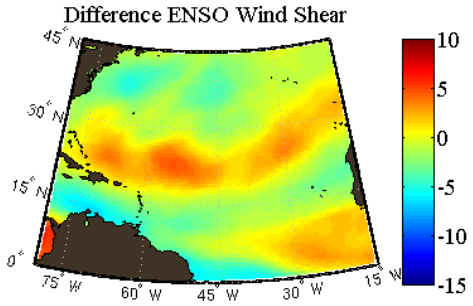

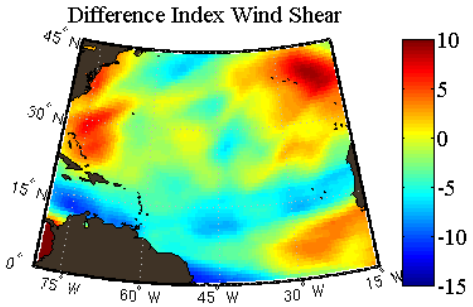

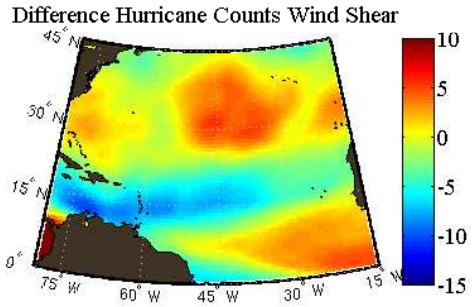

Figure 27: Diff Wind Shear

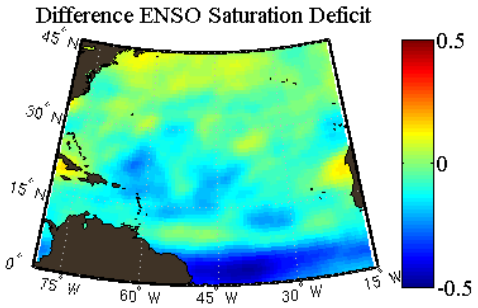

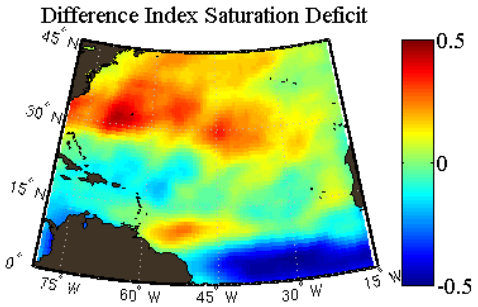

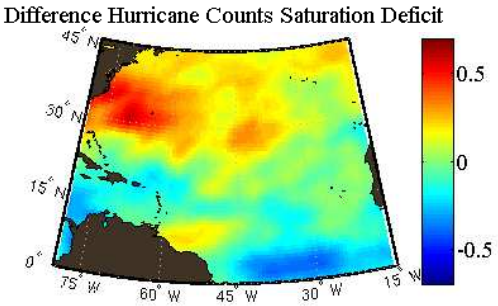

Figure 28: Diff Saturation Deficit

3 Average Difference Bar Graphs

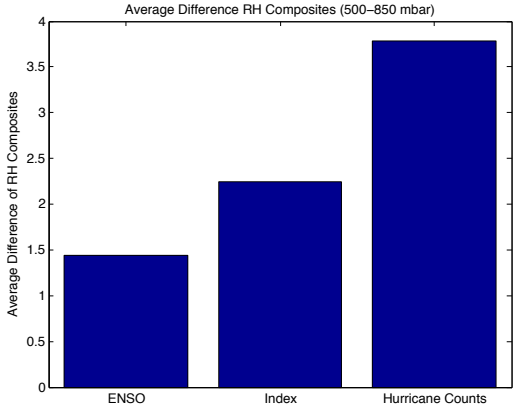

Figure 29: Avg Diff Relative Humidity

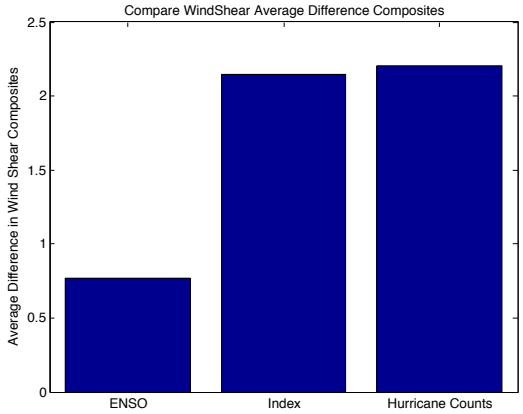

Figure 30: Avg Diff Wind Shear (between 850-200mbar)

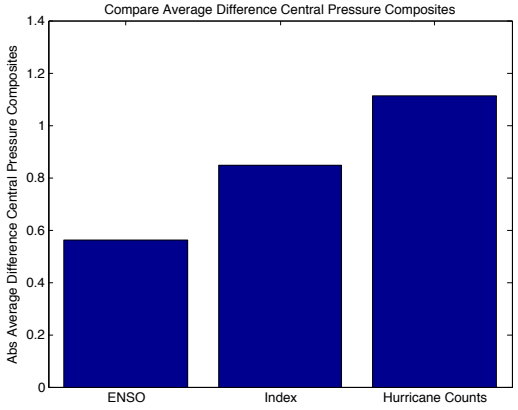

Figure 31: Avg Diff Central Pressure

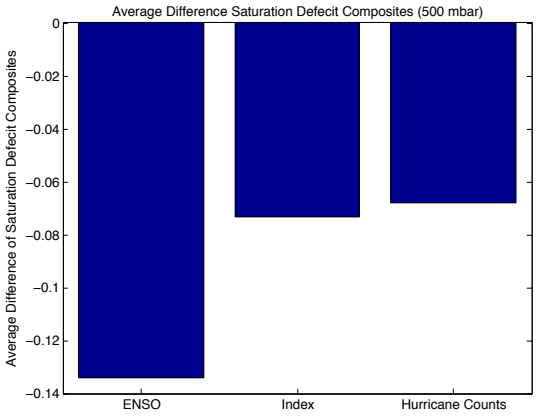

Figure 32: Avg Diff Saturation Deficit

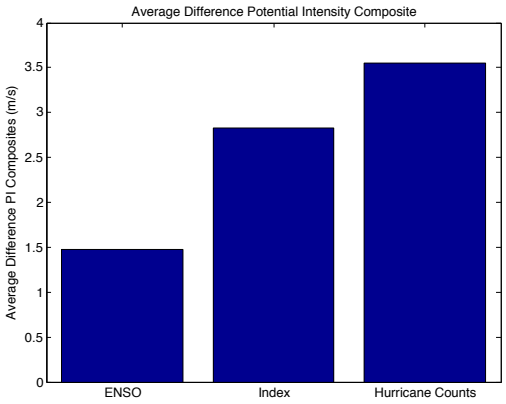

Figure 33: Avg Diff Potential Intensity

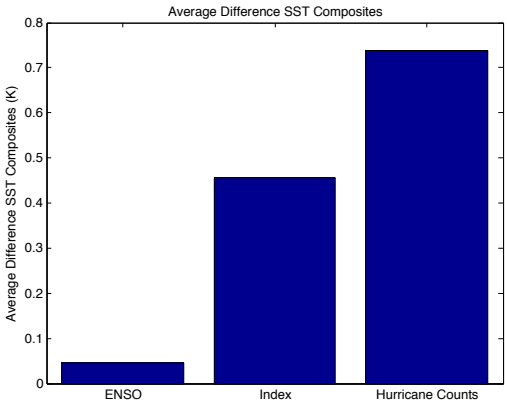

Figure 34: Avg Diff SST

References

[1] K. Ashok, S.K. Behera, S.A. Rao, H. Weng, and T. Yamagata. El niño modoki and its possible teleconnection. *J. Geophys. Res*, 112(10.1029), 2007.

[2] K. Ashok and T. Yamagata. The el nino with a difference. *Nature*, 461(7263), 2009.

[3] G D Bell, M S Halpert, R C Schnell, R W Higgins, J Lawrimore, V E Kousky, R Tinker, W Thiaw, M Chelliah, and A Artusa. Climate assessment for 1999. *Bulletin of the American Meteorological Society*, 81(6):S1–S50, 2000.

[4] M.C. Bove, J.J. O'Brien, J.B. Eisner, C.W. Landsea, X. Niu, et al. Effect of el nino on u. s. landfalling hurricanes, revisited. *Bulletin of the American Meteorological Society*, 79(11):2477–2482, 1998.

[5] J.B. Elsner, B.H. Bossak, and X.F. Niu. Secular changes to the ENSO-US hurricane relationship. *Geophysical Research Letters*, 28(21):4123–4126, 2001.

[6] Kerry Emanuel. Increasing destructiveness of tropical cyclones over the past 30 years. *Nature*, 436(7051):686–688, 2005.

[7] S.B. Goldenberg, C.W. Landsea, A.M. Mestas-Nuñez, and W.M. Gray. The recent increase in atlantic hurricane activity: Causes and implications. *Science*, 293(5529):474, 2001.

[8] W.M. Gray. Atlantic seasonal hurricane frequency. part i: El niño and 30 mb quasi-biennial oscillation influences. *Mon. Wea. Rev*, 112(9):1649–1668, 1984.

[9] Hye-Mi Kim, Peter J. Webster, and Judith A. Curry. Impact of Shifting Patterns of Pacific Ocean Warming on North Atlantic Tropical Cyclones. *Science*, 325(5936):77–80, 2009.

[10] B.P. Kirtman. Oceanic rossby wave dynamics and the enso period in a coupled model. *Journal of climate*, 10(7):1690–1704, 1997.

[11] P.J. Klotzbach. El niño-southern oscillation's impact on atlantic basin hurricanes and us landfalls. *Journal of Climate*, 24(4):1252–1263, 2011.

[12] H.L. Ren and F.F. Jin. Niño indices for two types of enso. *Geophysical Research Letters*, 38(4):L04704, 2011.

[13] D.M. Smith, R. Eade, N.J. Dunstone, D. Fereday, J.M. Murphy, H. Pohlmann, and A.A. Scaife. Skilful multi-year predictions of Atlantic hurricane frequency. *Nature Geoscience*, 3:846–849, 2010.

[14] D.M. Smith, A.A. Scaife, and B.P. Kirtman. What is the current state of scientific knowledge with regard to seasonal and decadal forecasting? *Environmental Research Letters*, 7:015602, 2012.

[15] BH Tang and JD Neelin. Enso influence on atlantic hurricanes via tropospheric warming. *Geophys. Res. Lett*, 31:L24204, 2004.

[16] K.E. Trenberth and D.P. Stepaniak. Indices of el niño evolution. *Journal of Climate*, 14(8):1697–1701, 2001.

[17] P.J. Webster and S. Yang. Monsoon and enso: Selectively interactive systems. *Quarterly Journal of the Royal Meteorological Society*, 118(507):877–926, 1992.

[18] A.T. Wittenberg. Are historical records sufficient to constrain enso simulations. *Geophys. Res. Lett*, 36:L12702, 2009.

[19] S.W. Yeh, J.S. Kug, B. Dewitte, M.H. Kwon, B.P. Kirtman, and F.F. Jin. El niño in a changing climate. *Nature*, 461(7263):511–514, 2009.